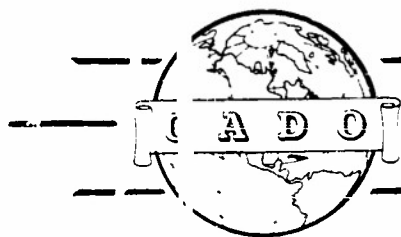


Reproduced by



CENTRAL AIR DOCUMENTS OFFICE

WRIGHT-PATTERSON AIR FORCE BASE - DAYTON OHIO

REEL-C

4005A

A. I. I

84239

The
U.S. GOVERNMENT

IS ABSOLVED

FROM ANY LITIGATION WHICH MAY ENSUE FROM ANY
INFRINGEMENT ON DOMESTIC OR FOREIGN PATENT RIGHTS
WHICH MAY BE INVOLVED.

UNCLASSIFIED

The Computation of Air Trajectories - and Appendixes A-C (Technical Report)

84 239

(None)

(Not known)

U.S. Air Force, Air Weather Service, Washington, D. C.

105-62

(Same)

June'50 Unclass. U.S. English 31 diagrs, graphs (Same)

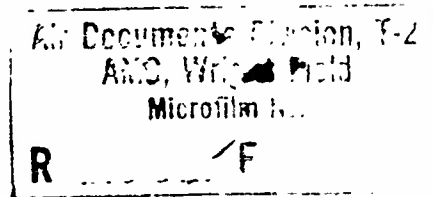
A critique has been made of the available methods of computing air trajectories, and a procedure which is the most accurate and feasible with the synoptic data generally available was determined. The notations which were followed and the applicable definitions are furnished. The discussion is centered on the computation and choice of thermodynamic trajectories, computation of isentropic trajectories using constant-pressure charts, comparison of alternate methods for computing isentropic trajectories, and trajectories of particulate matter. Attention is also given to the gradient-wind approximation, errors in computation of the Montgomery function, and a nomogram for obtaining the isentropic streamlines from the constant-pressure contours and isotherms.

Copies obtainable from CADO by U.S. Military Organizations only.

Meteorology (30)
Winds (5)

Winds - Measurement

Weather forecasting
Air - Physical properties



ATI No. 84 239

CARDO FILE COPY

UNCLASSIFIED

AIR WEATHER SERVICE
TECHNICAL REPORT 105-62

THE COMPUTATION OF
AIR TRAJECTORIES



JUNE 1950

HEADQUARTERS
AIR WEATHER SERVICE
WASHINGTON, D.C.

HEADQUARTERS
AIR WEATHER SERVICE
Andrews Air Force Base
Washington 25, D. C.

June 1950

Air Weather Service Technical Report 105-62, "The Computation of Air Trajectories," is published for the information and guidance of all concerned.

BY COMMAND OF BRIGADIER GENERAL YATES:

LEWIS L. MUNDELL
Colonel, USAF
Chief of Staff

OFFICIAL:

Robert B. Edwards
ROBERT B. EDWARDS
Major, USAF
Adjutant General

DISTRIBUTION: "E"
(1) ea. AWS Hq, A, B and C Detach.
(5) Hq, USAF
(20) Hq, AMC, MCLAWS
(20) Cambridge Research Laboratories
(10) C. G., Air University
(5) Chanute AFB
(10) U. S. Navy, Aerology
(10) U. S. Weather Bureau

PREFACE

From time to time Air Weather Service forecasters are required to compute air trajectories. The procedures for computing trajectories have not been adequately treated in the literature nor standardized among meteorologists. Major Arthur F. Gustafson of Headquarters, Air Weather Service has made a critique of the available methods and determined the procedure which is most accurate and feasible with the synoptic data generally available. His report, published herewith, is commended to all personnel concerned with the problem.

THE COMPUTATION OF AIR TRAJECTORIES

1. Notation. — The following notation will be used in this report:

p = atmospheric pressure.

T = atmospheric temperature.

θ = potential temperature.

θ_e = equivalent potential temperature.

g = acceleration of gravity.

c_p = specific heat at constant pressure.

$\gamma = - \frac{\delta T}{\delta z}$ = the lapse rate.

$\gamma_d = \frac{g}{c_p}$ = the dry adiabatic lapse rate.

2. Definitions. — For the purpose of this report the following definitions will apply:

a. The three-dimensional air trajectory is the curve in space described by the successive positions of an air parcel.

b. The two-dimensional air trajectory, hereafter referred to as an air trajectory, is the projection of a three-dimensional air trajectory onto a level surface.

c. The thermodynamic trajectory is the trajectory (2 dimensional) which an air parcel would follow if one of its thermodynamic parameters p , θ , or θ_e remained invariant. For example an isobaric (isentropic) trajectory is the thermodynamic trajectory the parcel would take if its pressure (entropy) remained invariant.

d. A thermodynamic surface is a surface along which, at each successive instant, a given thermodynamic parameter (e.g., p , θ , T , etc.) is constant. For example, an isobaric (isentropic) surface is one on which pressure (entropy) is constant.

e. A thermodynamic streamline is a curve which, at a given instant, is everywhere tangent to the direction of the wind projected onto a level surface from a given thermodynamic surface. If the winds are projected from an isobaric (isentropic) surface, the curve is called an isobaric (isentropic) streamline.

f. An isotachic surface is a surface on which, at a given instant, the magnitude of the horizontal component of the wind is everywhere the same.

g. An isobaric (isentropic) isotach is the projection onto a level surface of a three-dimensional isotach formed by the intersection of an isotachic surface with an isobaric (isentropic) surface.

3. Air Trajectories. — In order to compute air trajectories it would be necessary to know the actual vertical velocities occurring at

each map time. Since this is never the case in practice, thermodynamic trajectories which can be computed from available data must be used as substitutes for air trajectories. The approximation involved here depends, of course, on the thermodynamic trajectory chosen (isobaric, isentropic, etc.) and to what extent the atmospheric processes are actually isobaric, isentropic etc. However, regardless of the degree of approximation involved, the substitution of a thermodynamic trajectory for an air trajectory is the best that can be done under the circumstances.

4. The Computation of Thermodynamic Trajectories. —

a. Direct wind analysis. — If wind observations were available at regular intervals over a sufficiently dense network of stations, thermodynamic streamlines and isotachs for a specific thermodynamic surface could be obtained, provided the hypsography of that surface were known.

The hypsography of isobaric or isentropic surfaces can be obtained from the analysis of synoptic radiosonde observations provided, of course, the radiosonde network is sufficiently dense and the observational errors are not too great.

With the same degree of accuracy of the radiosonde observations, however, the hypsography of some thermodynamic surfaces can be determined more accurately than others. For example, the hypsography of an isobaric surface can be determined more accurately than that of an isentropic surface, the latter becoming quite inaccurate in case the prevailing lapse rate of temperature approaches that of the dry

adiabatic lapse rate. For this reason isobaric streamlines and isotachs can be determined more accurately than isentropic streamlines and isotachs if direct wind analysis is used. As will be pointed out in the next section, however, this is not the case when derived winds must be used.

Having obtained the thermodynamic streamlines and isotachs for the various map times t_0 , t_1 , t_2 , ..., t_n involved, the computation of the thermodynamic trajectory proceeds in the following manner: (see Fig. 1.)

(1). Beginning at the initial point P_0 the streamline through P_0 at t_0 is followed "forwards" for a distance $s_1 = V_0(t_1 - t_0)$, locating the point P_1 . (V_0 is the wind speed at P_0 at t_0 .)

(2). From P_1 the streamline through that point for the time t_1 is followed "backwards" for a distance $s_2 = V_1(t_1 - t_0)$ locating the point P_0' . (V_1 is the wind speed at P_1 at t_1)

(3). The vector $P_0'P_0$ is transferred to the point P_1 , locating the point P_2 .

(4). As a first approximation, a point Q_0 is located about halfway between P_1 and P_2 on the line joining them.

(5). Through the points P_0 and Q_0 a smooth curve is drawn tangent to the streamline for the time t_0 at P_0 and tangent to the streamline for the time t_1 at Q_0 .

(6). The distance along the newly constructed curve P_0Q_0 is then measured and compared with the distance $\bar{S} = \bar{V}(t_1 - t_0)$ (where

\bar{V} is the mean of the wind speed V_0 and the wind speed at Q_0 for the time t_1).

(7). If these distances are not in agreement, the position of Q_0 should be adjusted slightly and the steps (5) and (6) repeated for this new Q_0' , etc.

(8). Starting at the adjusted Q_0 the procedure (1) through (7) is repeated again using the charts for t_1 and t_2 , etc. Various other methods¹, whose accuracy is comparable to the one outlined above, may be employed. The accuracy of any method used, however, depends on the time interval between consecutive charts and on the accuracy with which the streamlines and isotachs can be drawn from the available wind observations.

b. Indirect wind analysis. — If wind observations sufficient in number to permit direct analysis of thermodynamic streamlines and isotachs are not available, these curves may be approximated by curves derived from the analysis of radiosonde observations. The isobaric streamlines, for example, can be represented by the contour lines of the constant pressure surface in question, the degree of approximation here being fairly well known. In the same way and to the same degree of approximation the isentropic streamlines may be represented by the isopleths of the Montgomery² function $\bar{\Phi} = Z_0 + \frac{C_p}{g} T_0$ (where Z_0 and T_0 are the height and temperature respectively of the isentropic

¹See for example Petterssen, Weather Analysis & Forecasting, Sec. 97, pp. 221-3.

²Montgomery, R. B., 1937; A Suggested Method for Representing Gradient Flow in Isentropic Surfaces. Bull. Amer. Met. Soc., June-July.

surface in question). The isobaric or isentropic isotachs may also be derived from the contours or from the isopleths of the Montgomery function as the case may be. The approximation usually made is the geostrophic wind approximation, in which case the isotachs obtained in either case represent the true isobaric or isentropic isotachs to the same degree of approximation.

Some improvement in the representativeness of derived wind speeds might accrue by using the gradient wind instead of the geostrophic wind³. As in the case of the geostrophic wind, the gradient wind speeds computed either from the isobaric contours or from the Montgomery stream-function lines represent the actual wind speeds to about the same degree of approximation. Insofar as an isentropic trajectory is a better estimate of the true trajectory than an isobaric trajectory, the computation of the gradient wind using the isentropic streamlines and their local rates of turning should yield slightly better approximations than the isobaric streamlines and their turning. Actually, in view of the other approximations made in deriving gradient wind formulae, the slight theoretical difference involved here has little practical significance.

5. The Choice of a Thermodynamic Trajectory. — As previously mentioned, the computation of air trajectories can not be carried out in

³A review of the assumptions involved in deriving a practical gradient wind formula is given in Appendix A.

practice. Thermodynamic trajectories using either wind observations, derived winds, or a combination of both must therefore be used as a substitute. Since constant pressure charts are drawn for other purposes, the computation of isobaric trajectories involves the least amount of additional work. If, however, the purpose is to find a thermodynamic trajectory which will most nearly approximate an air trajectory, an isentropic trajectory would probably be the better choice. A still better choice, from a purely theoretical point of view, would be a constant θ_e (equivalent potential temperature) trajectory. Practical considerations such as the uncertainties involved in humidity measurements, however, rule out this choice as being not worth the added complexity it entails.

Having determined to use isentropic trajectories as approximate air trajectories, it does not follow that it is necessary to draw isentropic charts. Isentropic trajectories may be computed using constant-pressure charts exclusively provided the latter are drawn at sufficiently close pressure intervals. Considering the fact that constant-pressure charts are required for other purposes and must therefore be drawn anyway, the possibility of computing isentropic trajectories in this way should be seriously considered.

6. The Computation of Isentropic Trajectories Using Constant Pressure Charts. — The vertical component of large-scale atmospheric motions is usually very small compared to the horizontal component. For short time intervals, therefore, air trajectories can be estimated by isobaric trajectories. For trajectories extending over several days,

however, the cumulative effect of even small vertical velocities⁴ may bring the air parcel to levels having completely different wind regimes from that of the initial level. An extended trajectory, therefore, cannot be estimated by a single extended isobaric trajectory. It may, however, as we shall see, be estimated by a series of short isobaric trajectories, each at a level corresponding to the approximate height of the parcel during the interval in question. The computation of trajectories in this step-wise fashion is carried out as follows:

(1). A short-period isobaric trajectory for the constant pressure surface $p = p_0$ is computed as usual.

(2). An assessment is made of the vertical motion⁵ which an air parcel traversing the two-dimensional trajectory (1) would experience if its potential temperature remained constant.

⁴Recent investigations (Miller, Studies of Large-Scale Vertical Motions in the Atmosphere, New York Univ., Met. Papers; Vol. 1, No. 1, 1948) have shown that the vertical component of large-scale currents is of the order of 1 cm/sec and rarely exceeds 0.1 m/sec. The sign of the vertical component, however, is often persistent over periods of 12 hours or more, with the result of that vertical amplitude of the trajectory can be of the order of 3 km. (i.e., 10,000 ft.).

⁵It can be shown that:

$$\Delta z \approx \frac{T_1 - T_2}{(\gamma_d - \gamma_2)}$$

where T_1 is the temperature at the beginning, and T_2 and γ_2 are the temperature and lapse rate at the end, of the isobaric trajectory.

(3). The pressure $p_0 + \Delta p$ corresponding to the height change Δz found in (2) is determined and the next short-period isobaric trajectory is computed for the constant pressure surface $p = p_0 + \Delta p$.

(4). Continuing in this manner a series of short isobaric trajectories, each for a different constant-pressure surface, is obtained, which series is equivalent to an extended isentropic trajectory.

The above outlined procedure is based on the assumption that the time intervals in question can be made arbitrarily small. In practice, however, the time intervals can not be arbitrarily chosen but are determined by the time interval between radiosonde observations. Since this is usually not less than 12 hours, small but significant deviations between the isobaric and isentropic trajectories might occur in some cases. A good approximation of the direction and magnitude of these deviations, however, can be computed by making use of the isobaric isotherms. A detailed outline of the procedure to be followed in making such computations is given in Appendix B.

In general the pressure levels p_0 , $p_0 + \Delta p$, etc., would not be standard pressure levels. In most cases, however, not much error would result, if the nearest standard pressure level were substituted for the computed level in each instance. An additional assumption involved in doing this, however, is that the vertical motion through the layer between the standard surface and the exact pressure surface is

fairly uniform so that the vertical motion assessed at the standard level applies also at the intermediate one.

In many instances the same standard level would have to be used for more than one consecutive 12-hour interval. For each interval, however, the vertical motion is assessed and added to the previous height so that the proper pressure height is always known. As soon as this pressure comes within 50 mb of the next standard level this level is used for the succeeding interval and so on.

If the air parcel is in a region with strong vertical shear (for example in a frontal zone) significant errors in the computation of its trajectory might result due to using a standard level which is 40 or 50 millibars from the correct level. In such cases, intermediate constant-pressure charts could be constructed or local isentropic stream-function charts could be used temporarily during the period the parcel is in such a region.

7. Comparison of Alternate Methods for Computing Isentropic Trajectories. — In the preceding section a method was given for computing isentropic trajectories using the contour lines of appropriate constant-pressure surfaces. Another more direct method, once the basic charts are constructed, is to use the Montgomery-function isopleths. Isentropic charts, however, are not regularly prepared for other purposes, whereas contour charts are. Furthermore, the computation of the Montgomery functions to be plotted at each radiosonde station entails a considerable amount of work, especially if it is to be done on a hemispherical basis. The question is: "Which method would be the more

efficient, (1) a fairly simple, direct one requiring tedious preparation of additional charts, or (2) an indirect, more involved one, using charts which are already available?" This question can be answered only through trial in the analysis centers and no attempt will be made to answer it here. Certain considerations concerning the comparative accuracies of the two methods, however, can be discussed and will certainly have a bearing on the ultimate choice of a standard method.

As previously mentioned, the hypsography of an isentropic surface can not be determined as accurately as that of an isobaric surface⁶. Winds plotted on an isentropic chart are therefore subject to height errors which are much larger (e.g., 1000 - 2000 feet) than those for winds plotted on constant-pressure charts. For this reason, wind directions plotted on an isentropic chart are apt to be less of an aid in drawing stream-function lines than are wind directions plotted on a constant-pressure chart in drawing contours. In the preparation of the basic charts to be used, therefore, the contour method has an advantage over the stream-function method.

As for the accuracy of the computed Montgomery-function values compared to that of the contour heights, it can be shown that one is as accurate as the other⁷. Except for the aid given by wind observations, therefore, the Montgomery-function lines of an isentropic surface can be drawn to the same degree of accuracy as the contour lines of a constant-pressure surface.

⁶As shown in Appendix C the height error Δz due to a temperature error ΔT is given by $\Delta z = \Delta T / (\gamma_d - \gamma)$.

⁷See Appendix C.

Because of the errors involved in determining the height of an isentropic surface, fairly large errors can be expected in the determination of the height of the hypothetical air parcel in question. Assuming that the parcel maintains its potential temperature, however, the error due to this indeterminacy is not cumulative. If, for example, a computed trajectory (2-dimensional) were exact the probable height error on the last day would be the same as that on the first day. Inasmuch as the height changes of the parcel are determined by reference to the height of a particular isentropic surface, both in the Montgomery-function method and the constant-pressure method, one method is as good (or bad) as the other in this respect also.

In view of the foregoing comparisons, it is obvious that the main differences in accuracy between the two methods, if any, would be due to the use (in the constant pressure method) of the nearest standard pressure level in place of the pressure level indicated from the height changes computed assuming adiabatic motion⁸. This difference, too, could be eliminated by drawing intermediate constant-pressure charts whenever necessary. How often intermediate charts would have to be drawn and which method is, in the last analysis, the more efficient, are questions which can not be answered except by those assigned to the job of making trajectory computations. There is, of course, also the

⁸In making this statement it is assumed that the slight differences between 12-hour isentropic and isobaric trajectories can be taken care of by the method given in Appendix B.

possibility that in some instances one method may be more efficient than the other while in other instances the reverse might be true. In such a case there is no reason why either method should have to be used to the exclusion of the other.

8. Trajectories of Particulate Matter. — The computation of the trajectories of particulate matter suspended in the air is further complicated by the combined effect of vertical shear and diffusion.

Consider for example, the case (Fig. 2) of a vertical column (AB) of air into which particulate matter has been injected. Suppose that the lower portion of the column moves along a trajectory AA' and the upper portion during the same time interval along a trajectory BB'. The column of particulate matter (without diffusion) would then arrive at the position A'B', no longer vertical, but tilted as illustrated. Due to vertical mixing, convection, etc., the particulate matter would be distributed along the vertical as shown by the vertical hatching in Figure 2. Simultaneously, horizontal mixing would have distributed the matter horizontally. Thus, particulate matter injected into the vertical column at AB in Figure 2 would at a later time be found in a wide area around the line A'B', the horizontal projection of which could easily be several thousand kilometers.

Now, if the problem is merely to detect matter which has been injected in a vertical column at a known source, very large errors in the computation of air trajectories can be tolerated due to the phenomena of spreading just described. On the other hand, if the problem is to compute the position of the unknown source from which detected

matter has originated, the large errors inherent in all current methods, coupled with the uncertainty that exists in regard to the influences of vertical velocity and vertical diffusion, are very likely to make the results unsatisfactory.

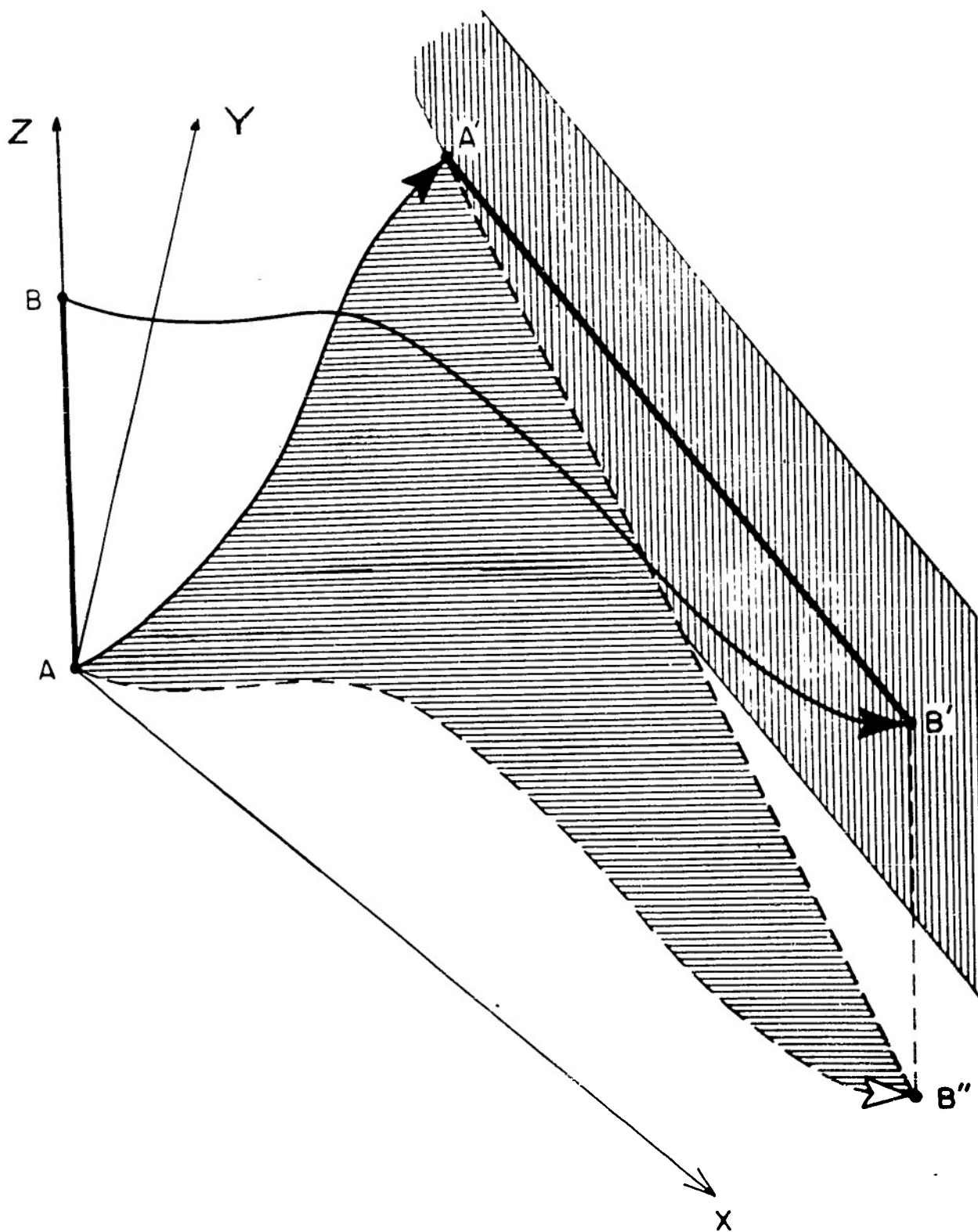


Fig.2 ILLUSTRATING THE EFFECT OF VERTICAL WIND SHEAR IN SPREADING OUT PARTICULATE MATTER INJECTED INTO A VERTICAL COLUMN.

APPENDIX A

The Gradient-Wind Approximation.

1. Notations:

The following notation will be used in this appendix in addition to that listed in item 1 of the basic report:

v = the horizontal wind vector,

V = the horizontal wind speed,

w = the vertical wind speed,

v_g = geostrophic wind velocity,

V_g = geostrophic wind speed,

G = the gradient wind speed,

ψ = the wind direction measured counterclockwise from due east,

ψ_g = the geostrophic wind direction,

$\beta = \psi - \psi_g$ is the angle of geostrophic deviation,

$\kappa = \frac{v}{V} \cdot \nabla \psi$ is the curvature of the wind streamlines,

$\kappa_g = \frac{v_g}{V_g} \cdot \nabla \psi_g$ is the curvature of the geostrophic wind streamlines,

$f = 2 \Omega \sin \phi$ is the Coriolis parameter, and

a = the radial distance to the center of the earth.

2. Approximations and assumptions. — Very often in practice wind soundings are too sparse to permit a direct analysis of the wind field, whereas sufficient data are available to compute the geostrophic wind field. In this case an approximate wind field can be derived from the geostrophic wind field and the computation of thermodynamic trajectories carried out in the same manner as outlined in paragraph 4a of the basic report except that derived streamlines and isotachs are used in place of the actual ones.

Various approximations to the actual wind can be made from the geostrophic wind field depending on the nature of the assumptions made. One assumption, however, is common to all approximations for winds at upper levels, viz., that the effects of friction can be neglected. Another assumption which is usually made is that the wind direction is instantaneously the same as the geostrophic wind direction, in which case we speak of the motion as being "gradient." Whereas the assumption of frictionless flow is probably a good one for upper levels, the gradient-wind assumption may, in some cases, introduce fairly large errors not only in the wind directions but in the wind speeds as well.

In a recent paper¹, Petterssen has derived an expression which relates the angle of geostrophic deviation to certain properties of

¹On the Sensitivity of the Wind Field to Pressure Variations, Tellus, Vol. 2, No. 1, Feb., 1950, pp 18-23.

the pressure field. It is shown, in this paper that large angles of geostrophic deviation β , may derive (a) from isallobaric gradients, (b) from convergence or divergence of the isobars, and (c) from the combined effects of (a) and (b). This angle of deviation is increased when the geostrophic shear is anticyclonic and decreased when it is cyclonic.

The assumption of frictionless gradient flow, however, is still insufficient to determine the wind speed and some further assumption regarding the curvature of the air trajectory must be made. Various assumptions concerning this curvature are used in practice, a few examples of these being:

- (a) The trajectory curvature is zero.
- (b) It is the same as that of the geostrophic streamlines (i.e., the pressure contour lines).
- (c) It is the same as the curvature of the isentropic trajectory which a hypothetical air parcel would take if its motion were, at all times, gradient.

Assumption (a) is the geostrophic-wind assumption and the wind speed obtained using it is the geostrophic wind speed. Assumption (b) is, in general, no better than (a) and only serves to make the computations more complicated. Assumption (c) yields results which are probably somewhat better than (a), especially for those cases where large trajectory curvatures are involved. In any case, we will use it as the best one possible.

3. The isentropic gradient-wind formula. — The so-called "normal" equation of motion for isentropic frictionless flow can be written:

$$(1) \quad A'V^2 + B'V - 2\Omega w \cos \vartheta \sin \Psi = fV_g \cos \Psi$$

where

$$A' = K + \frac{\tan \vartheta}{a} \cos \Psi ,$$

$$B' = f + \frac{\partial \Psi}{\partial t} .$$

(K and $\frac{\partial \Psi}{\partial t}$ are here the curvature and local rate of turning,

respectively, of the isentropic streamlines.)

The term $2\Omega w \cos \vartheta \sin \Psi$, which is the Coriolis force due to the vertical motion, is ordinarily very small compared to the other terms in (1) and may therefore be neglected. Furthermore under the assumption (c) above $\Psi \cong \Psi_g$ and therefore $K = K_g$, $\frac{\partial \Psi}{\partial t} = \frac{\partial \Psi_g}{\partial t}$ and $\cos \vartheta = 1$.² Equation (1) may therefore be written:

$$(2) \quad AG^2 + BG = fV_g ,$$

where: $A = K_g + \frac{\tan \vartheta}{a} \cos \Psi_g ,$

$$B = f + \frac{\partial \Psi_g}{\partial t} .$$

² K_g and $\frac{\partial \Psi_g}{\partial t}$ are here the curvature and local rate of turning respectively of the isentropic geostrophic streamlines (i.e., the Montgomery-function isopleths.)

Equation (2) is quadratic and has the two solutions

$$G_1 = \frac{-B + \sqrt{B^2 + 4AfV_g}}{2A} ,$$

$$G_2 = -G_1 - \frac{B}{A} .$$

The solution G_2 may apply in some cases to winds which occur locally in large and medium-scale pressure systems, notably to the right of the path of anticyclonic centers and in connection with strongly curved wedges in the upper troposphere in middle latitudes. It also applies to small-scale wind disturbances such as dust whirls and tornadoes but this is of no interest here. For most large-scale winds occurring at upper levels, however, the solution G_1 is applicable and is the one which should be used in computing the wind from the pressure of contour fields alone. In making computations of G_1 in practice, tables or nomograms should be constructed giving G_1 as a function of ϕ , ψ_g , $\frac{\partial \psi_g}{\partial t}$, K_g , and V_g . Except when V_g is very large the term $\frac{\tan \phi}{a} \cos \psi_g$ in A may be neglected.* In some cases G_1 may turn out to be a complex number in which case the best that can be done is to use the real part.

If the geostrophic streamlines under consideration move without appreciable alteration of their shape, the local turning of the geostrophic streamlines may be approximated by: $\frac{\partial \psi_g}{\partial t} = -K_g C \cos \alpha$,

* If K_g is measured by fitting an arc on a Lambert conformal map the term $\frac{\tan \phi}{a} \cos \psi_g$ is automatically included and should not be added to K_g .

where: C is the speed of the geostrophic streamline configuration
 and α is the angle from the direction of motion of the
 system to the geostrophic wind direction at the point
 considered.

A discussion of the application of the wind-speed formula derived
 using this alternative form for the turning of the wind can be found
 in the paper, "Computation of Winds in the Free Atmosphere."³

Equation (2) may also be applied to compute the isentropic
 gradient wind from constant pressure charts. In this case, however,
 if K_g and $\frac{\partial \psi_g}{\partial t}$ refer to the curvature and local rate of turning
 of the contours, the coefficients A and B must then be written:

$$A = K_g + \frac{\tan \alpha}{a} \cos \psi_g - \frac{g}{fV_g} \frac{\left(\frac{\partial T_p}{\partial s_g}\right)^2}{T(\gamma_d - \gamma)},$$

$$B = f + \frac{\partial \psi_g}{\partial t} - \frac{g}{fV_g} \frac{\left(\frac{\partial T_p}{\partial t}\right)\left(\frac{\partial T_p}{\partial s_g}\right)}{T(\gamma_d - \gamma)},$$

where:

T_p is the map of the temperature in the constant pressure
 surface,

³S. Petterssen, NAVAER No. 50-IR-166

$$\text{and } \frac{\partial T_p}{\partial s_g} = \frac{v_g}{V_g} \cdot \nabla T_p .$$

APPENDIX B

A Nomogram for Obtaining the Isentropic Streamlines from the Constant-Pressure Contours and Isotherms.

In a barotropic atmosphere an isentropic surface is coincident with an isobaric surface and the isentropic stream-function lines and the contour lines for this surface are the same. In a baroclinic atmosphere, however, the isentropic surface is inclined with respect to the isobaric surface and, although the stream function lines of an isentropic surface are tangent to the contour lines of an isobaric surface along the intersection of the two surfaces, they do not¹ remain tangent away from this intersection. Instead, the isentropic streamlines being more strongly curved anticyclonically (or less strongly curved cyclonically) deviate to the right of the contour lines as one proceeds along a contour in the direction of the geostrophic wind.

Consider now an isentropic stream-function line S_e and an isobaric contour S_p both through the point P_0 which lies on the line of intersection between the isentropic and isobaric surfaces from which S_e and S_p were projected. Assuming that the difference ΔK between the curvatures of S_e and S_p remains constant as one proceeds along S_p to a point P_1 , the distance Δy between S_e and

¹Except in the special case of horizontal barotropy.

S_p at P_1 would be given by:

$$\Delta y = \frac{\Delta K}{2} (\Delta x)^2$$

where Δx and Δy are measured as illustrated in Figure 3.

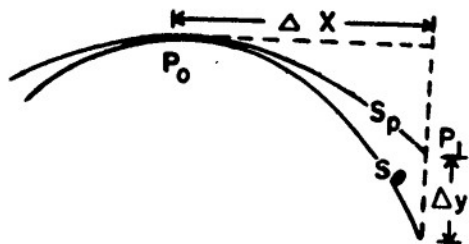


Fig. 3

It can be shown that the difference between K_e and K_p at P_0 is given by

$$K_e - K_p = \Delta K = - \frac{\left(\frac{\partial T_p}{\partial x} \right)^2}{\left(\frac{\partial z_p}{\partial y} \right) (\gamma_d - \gamma T_p)}$$

where:

z_p is the contour height,

T_p is the isobaric temperature, and

γ is the lapse rate, $\gamma_d = \frac{g}{c_p}$ is the dry adiabatic lapse rate.

If the further assumption is made that $\frac{\partial T_p}{\partial x}$ is constant, then:

$$\Delta y = \frac{-(\Delta T_p)^2}{2\left(\frac{\partial Z_p}{\partial y}\right)(\gamma_d - \gamma)T_p}, \quad (1)$$

where ΔT_p is the isobaric temperature difference between the points P_0 and P_1 .

If the contour interval is ΔZ_p and the spacing between contours in the Y direction is Δn equation (1) can be written

$$\Delta y = -\frac{1}{M}(\Delta T_p)^2 n, \quad (2)$$

where $M = 2\Delta Z_p(\gamma_d - \gamma)T_p$. (3)

A nomogram* giving Δy as a function of ΔM , Δn and ΔT_p is shown in Figure 4. The use of this nomogram in locating the point P_1' is illustrated by an example shown in Figure 5. The nomogram has supposedly been laid over a contour map for which only the contours

*This nomogram is independent of the map scale or the contour interval ΔZ_p . It should be noted, however, that M is proportional to the contour interval ΔZ_p . Values of M taken for a table prepared for a 100-ft interval must therefore be doubled when applied to a map with 200-ft contours.

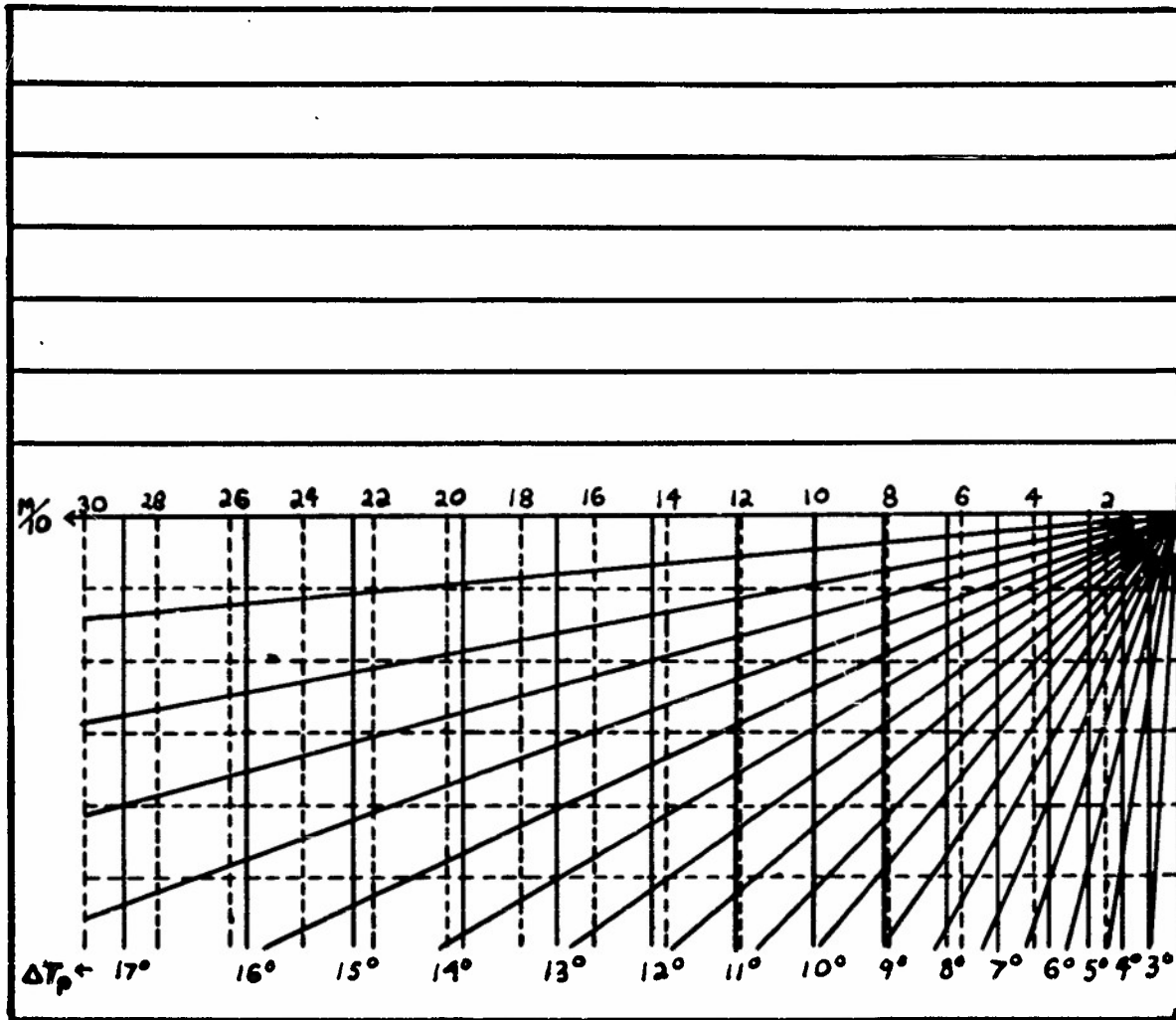


Fig. 4. Nomogram for determining the difference between isobaric and isentropic streamlines.

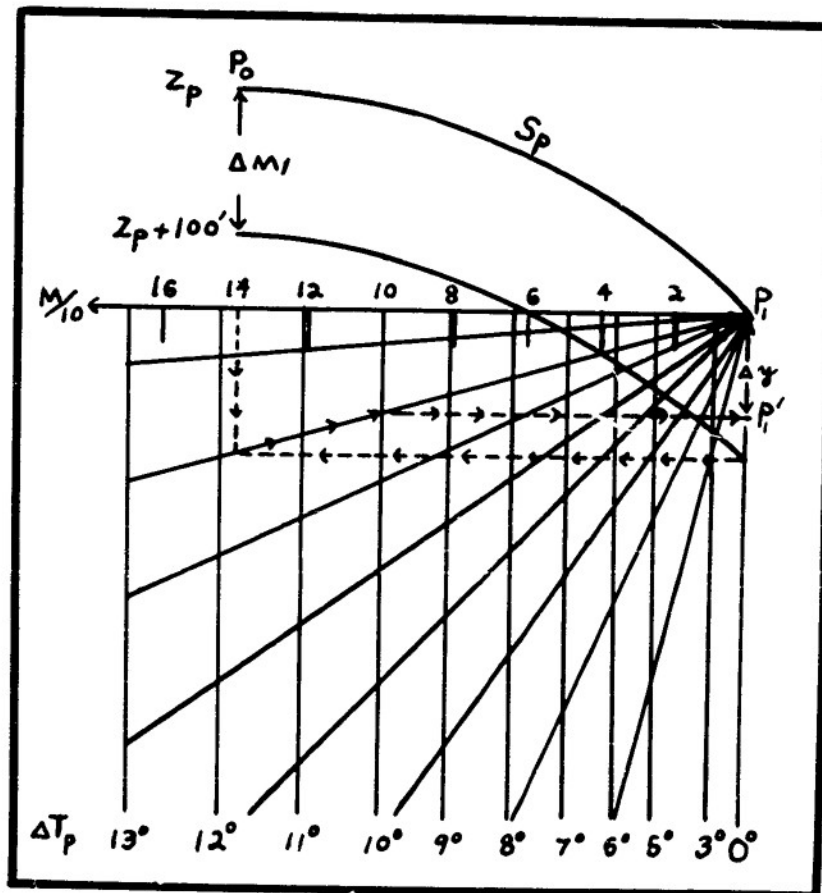


Fig. 5. Illustration of the use of nomogram (Fig. 4.).

Z_p and $Z_p + 100'$ are shown. The point $M = 0$, $Y = 0$ is placed at P_1 with the scale aligned in such a way that the tangent to S_p at P_0 is parallel to the M axis. Let us suppose that $\Delta T_p = 10^\circ \text{C}$ and that M is 140 deg^2 . The manner in which Δy is then found is as follows:

(1). The $M = 140 \text{ deg}^2$ line is followed to its intersection with the $\Delta n = \Delta n_1$ line, where Δn_1 is the distance between the contours Z_p and $Z_p + 100'$, as shown.

(2). The diagonal line $\frac{\Delta n}{H} = \text{const.}$, through this intersection is then followed until it intersects the $\Delta T = 10^\circ \text{C}$ Line.

(3). The $Y = \text{constant}$ line through the intersection (2) is then followed back to the Y axis locating the point P_1' .

In the above example Δn_1 , is measured at P_1 rather than at P_0 as indicated by the derivation of equation (2). This permits more convenient use of the scale and the difference involved should in most cases be small. If, however, the difference between these spacings is considerable, an average value of Δn should be used. Strictly speaking, the value of M should also be a mean of its values at the points P_0 and P_1 . The difference here, however, would in most cases be insignificant, especially in view of the fact that Δy is usually a very small correction anyway.

Having found the point P_1' , a smooth curve S_e' beginning at P_0 and tangent to the contour line S_p there, is drawn to the point P_1' in such a way that the deviation between S_e' and S_p increases

regularly from P_0 to P_1' . The curve S_0' is then taken as a first approximation to the isentropic streamline S_0 through P_0 and is used instead of S_p in the computation of the trajectory.

APPENDIX C

Errors in Computation of the Montgomery Function.

The Montgomery functions:

$$\bar{\Phi} = Z_0 + \frac{C_p}{g} T_0$$

is computed from the radiosonde report as follows: (see Fig. 6)

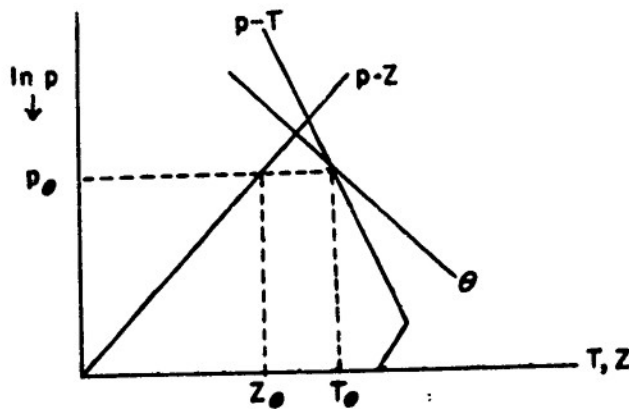


Fig. 6

(a) The intersection of the θ line in question with the $p - T$ curve is located and the temperature T_0 is read off at this point.

(b) The height Z_0 corresponding to pressure p_0 is found from the pressure-height curve.

(c) Z_0 is added to T_0 multiplied by $\frac{C_p}{g}$.

Let us now suppose that the $p - T$ and the $p - Z$ curves observed are slightly erroneous due to observational errors. The error in the determination of Z_0 will then be due to:

(a) The error Δp_0 in obtaining p_0 from the erroneous $p - T$ curve. (See Fig. 7.)

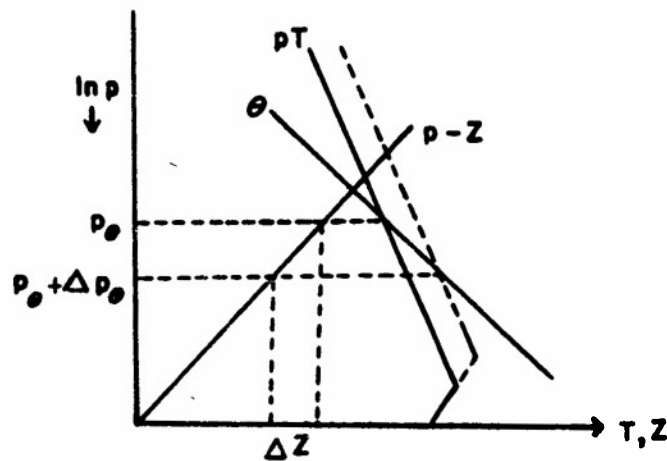


Fig. 7

(b) The error in obtaining the height from the erroneous $p - Z$ curve, corresponding to the pressure $p_0 + \Delta p_0$.

It will be shown that the error due to (a) is cancelled exactly by the error in the expression $\frac{C_p T_0}{g}$ and that for this reason the total error in $\bar{\Phi}$ is due only to that mentioned in (b).

Now p_0 and T_0 are related by the expressions:

$$\ln \theta = \ln T_0 - \frac{R}{C_p} \ln \frac{p_0}{100} = \text{const.}$$

Thus:

$$\frac{C_p}{g} \Delta T_o = \frac{RT_o}{gP_o} \Delta P_o .$$

But the error in Z_o due to (a) above is just:

$$\Delta Z = - \frac{1}{g} \int_o \Delta p_o = - \frac{C_p}{g} \Delta T_o$$

and therefore cancels the error $+ \frac{C_p}{g} \Delta T_o$ due to an erroneous determination of T_o .

The error ΔZ in computing the height of the isentropic surface, however, is not canceled by a compensating error. Assuming a constant lapse rate γ the error ΔT_o due to a constant temperature error ΔT is given by: (See Fig. 8)

$$T_o = \frac{\gamma_d}{\gamma_d - \gamma} \Delta T \quad (\text{where } \gamma_d = \frac{g}{C_p}) .$$

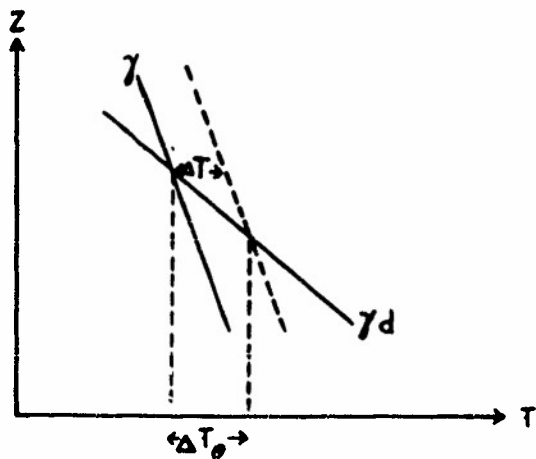


Fig. 8

The height error is therefore:

$$\Delta z = \frac{\Delta \bar{T}}{\gamma_d - \gamma} = \frac{c_p}{g} \Delta T / \left(1 - \frac{\gamma}{\gamma_d}\right).$$

For $\frac{\gamma}{\gamma_d} = 3/4$, for example, a temperature error of 1°C will result in a height error of 400 meters (approx. 1300 ft).

Thus it is seen that whereas the error in the computation of the Montgomery function is no greater than the error in the computation of the height of a constant pressure surface, the error in computing the height of an isentropic surface may be quite large.

Reproduced by



CENTRAL AIR DOCUMENTS OFFICE

WRIGHT-PATTERSON AIR FORCE BASE - DAYTON, OHIO

REEL-C

4005A

A.T.I

84239

The
U.S. GOVERNMENT

IS ABSOLVED

FROM ANY LITIGATION WHICH MAY ENSUE FROM ANY
INFRINGEMENT ON DOMESTIC OR FOREIGN PATENT RIGHTS
WHICH MAY BE INVOLVED.

UNCLASSIFIED